

X-RayVision-Net: CBAM-Infused YOLOv8 for Rapid Pulmonary Disease Recognition

Louis Mario Wijaya ¹, Daniel Martomanggolo Wonohadihjojo ^{1,*}

¹ Universitas Ciputra, Indonesia

* Corresponding author: Daniel Martomanggolo Wonohadihjojo, Universitas Ciputra, Indonesia
✉ daniel.m.w@ciputra.ac.id

Copyright: © 2026 by the authors

Received: 25 October 2025 | Revised: 25 November 2025 | Accepted: 16 Desember 2025 | Published: 17 February 2026

Abstract

Tuberculosis and pneumonia continue to pose major global health challenges, particularly in regions with limited radiological resources, where overlapping chest X-ray patterns often complicate differential diagnosis. This study proposes X-RayVision-Net, a hybrid deep learning framework that integrates the Convolutional Block Attention Module (CBAM) into the YOLOv8 architecture to enhance pulmonary disease classification. A quantitative experimental design was employed using 10,056 chest X-ray images categorized as normal, pneumonia, or tuberculosis, collected from multiple public datasets. Image preprocessing involved Contrast Limited Adaptive Histogram Equalization (CLAHE) and balanced data augmentation to improve visual consistency and address class imbalance. The proposed model was trained for 100 epochs and evaluated against a standard YOLOv8 baseline using accuracy, precision, recall, and F1-score. Experimental results demonstrate that the CBAM-enhanced YOLOv8 model achieved an accuracy of 98.99%, outperforming the baseline model (97.37%) and yielding consistent improvements across all performance metrics. The findings confirm that the incorporation of channel and spatial attention mechanisms effectively refines pulmonary feature representation, facilitating more accurate discrimination between tuberculosis and pneumonia. This framework presents a rapid and reliable computer-aided diagnostic approach suitable for deployment in clinical environments with constrained radiology expertise.

Keywords: cbam; computer-aided diagnosis; deep learning; lung disease classification; yolov8

To cite this article: Wijaya, L. M., & Wonohadihjojo, D. M. (2026). X-RayVision-Net: CBAM-Infused YOLOv8 for Rapid Pulmonary Disease Recognition. *Edumatic: Jurnal Pendidikan Informatika*, 10(1), 1–10. <https://doi.org/10.29408/edumatic.v10i1.32784>

INTRODUCTION

Tuberculosis (TB) is a chronic infectious disease caused by *Mycobacterium tuberculosis*. It primarily affects the lungs regardless of age or gender and is notoriously difficult to treat due to the bacterium's resilience and ability to persist in the body for long periods (Suvvari, 2025). In addition to TB, another major respiratory infection with significant global impact is pneumonia. Pneumonia affects the alveoli and can be triggered by bacteria, viruses, or fungi, leading to inflammation and fluid accumulation that cause breathing difficulties. *Streptococcus pneumoniae* is the most common bacterial cause, although other pathogens such as *Mycoplasma*, *influenza* viruses, and coronaviruses can also be responsible (Hekmatyar et al., 2022; Yu et al., 2025).

Indonesia accounted for approximately 10% of global TB cases in 2023, ranking second after India as the country with the highest TB burden worldwide (Alfaqeeh et al., 2025; Firdaus



et al., 2025). Pneumonia likewise remains a serious health threat among children in Indonesia and is one of the leading causes of death among infants and toddlers (Ciptaningtyas et al., 2025; Umar et al., 2024). Early detection of tuberculosis and pneumonia is crucial, as both diseases often exhibit similar clinical symptoms despite requiring distinctly different treatments. However, the limited number of trained medical professionals and the challenges of interpreting chest radiographs, due to overlapping visual patterns between the two diseases and inconsistent image quality, often make manual diagnosis slow and less accurate (Pal et al., 2024). These challenges have motivated the development of computer-aided diagnostic (CAD) systems powered by deep learning technologies. Deep learning, a subfield of machine learning, mimics the way the human brain processes information through artificial neural networks. It operates by learning simple patterns first and then combining them to form higher-level representations. In other words, deep learning builds complex knowledge from simple features and uses what it learns to better recognize smaller details more accurately (Alzubaidi et al., 2021; Theotokis, 2025).

To address the challenges of manual diagnosis and inconsistent image quality, the proposed solution leverages recent advances in deep learning. One of the most common architectures, the Convolutional Neural Network (CNN), has achieved an accuracy of 97% in classifying COVID-19, viral pneumonia, and lung opacity (Karim et al., 2024). However, to achieve faster and more efficient detection, significant progress has been demonstrated by the You Only Look Once (YOLO) family of architectures. Among its latest iterations, YOLOv8 has emerged as a state-of-the-art (SOTA) model supporting various vision AI tasks (Khalaf & Abdulateef, 2024). The theory behind YOLOv8's effectiveness lies in its single-stage detection capability, which allows for rapid image processing without sacrificing accuracy.

YOLOv8 has demonstrated remarkable versatility and high performance across various medical imaging disciplines. In fundus image-based eye disease classification, YOLOv8 achieved 92% accuracy (Muhlashin & Stefanie, 2024), while another ophthalmology study reached 94% accuracy (Khalaf & Abdulateef, 2024). In blood cell analysis, YOLOv8 obtained 99.982% accuracy on the Acute Lymphoblastic Leukemia (ALL) dataset (Nunes et al., 2025). Similarly, in skin disease classification, the model recorded a precision of 85.33% (Pradeepa et al., 2024). Despite these successes, standard CNN and YOLO architectures treat all image regions with equal importance, often missing subtle disease patterns in complex lung X-rays.

To overcome the limitations of uniform feature processing and prioritize clinically relevant regions, this study incorporates the Convolutional Block Attention Module (CBAM). CBAM enhances the network's ability to highlight informative visual features by combining channel and spatial attention. Previous studies have demonstrated CBAM's efficacy in detecting focal abnormalities, achieving high accuracy in brain tumor classification (Oladimeji & Ibitoye, 2023), and skin cancer detection (Priambodo & Faticahah, 2025). Within YOLO-based architectures, attention mechanisms have also shown promise, such as in pediatric bronchoscopy object detection (Yan et al., 2024).

Despite these advancements, most existing implementations predominantly target the detection of distinct, well defined lesions such as tumors or are limited to single-domain applications. Consequently, they are less effective in addressing the diagnostic complexity of differentiating tuberculosis and pneumonia, conditions characterized by diffuse and overlapping pulmonary infiltrates rather than clearly delineated masses. Moreover, the integration and complementary potential of the state-of-the-art YOLOv8 architecture with the Convolutional Block Attention Module (CBAM) for this challenging differential diagnosis in chest X-ray imaging have received limited systematic investigation in the existing literature.

Consequently, this study focuses on integrating the CBAM attention mechanism into the YOLOv8 architecture to address the specific complexities of distinguishing between tuberculosis and pneumonia. We propose a hybrid model specifically optimized to prioritize

clinically relevant pulmonary features, rigorously evaluating its performance against standard baselines. By enhancing feature extraction and classification accuracy, this work establishes a robust diagnostic tool intended to support early disease identification in healthcare settings with limited radiological resources.

METHOD

This quantitative study utilizes a CBAM-infused YOLOv8 architecture for lung disease classification, developed within Visual Studio Code. As depicted in Figure 1, the study adopts a systematic five-stage pipeline designed to ensure data integrity and rigorous validation. The process begins with dual-source Dataset Collection, followed by enhancement-focused Data Pre-processing using CLAHE and augmentation. Subsequently, Data Splitting ensures class balance prior to the Model Construction & Training phase. The workflow concludes with Model Evaluation, employing performance metrics and confusion matrices to quantitatively assess the attention mechanism's impact.

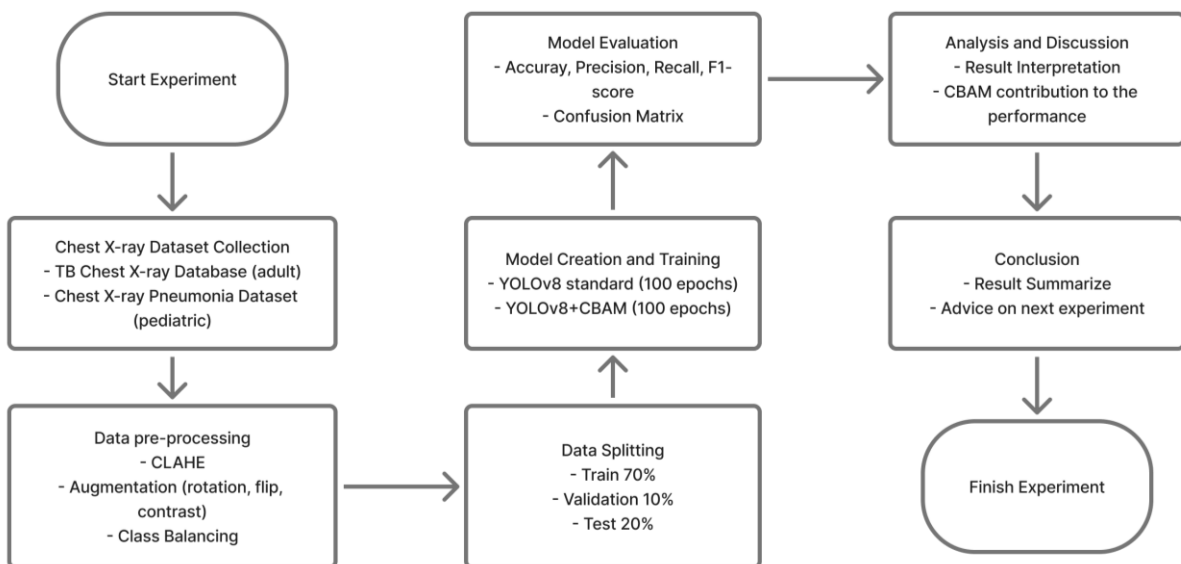


Figure 1. Sequential research workflow for lung disease classification.

Following the initial "Dataset Collection" phase outlined in Figure 1, this study aggregates data from two distinct public repositories to ensure a diverse and balanced training set. The primary source is the Tuberculosis (TB) Chest X-ray Database, which includes 700 TB-positive and 3,500 normal images (Hadhou et al., 2024). This is complemented by the Chest X-ray Pneumonia dataset from Guangzhou Women and Children's Medical Center, which includes 5,856 pediatric X-rays with 4,273 pneumonia and 1,583 normal cases (Hadhou et al., 2024). Consequently, 10,056 pictures totaling 700 TB, 4,273 pneumonia, and 5,083 normal cases were acquired after combining the two datasets; bacterial and viral pneumonia were merged into a single class. Images were randomly split into training (70%), testing (20%), and validation (10%) subsets while preserving class balance. Since all datasets were anonymized and made public, ethical approval was not required. Contrast Limited Adaptive Histogram Equalization (CLAHE) was used in preprocessing to improve picture quality and make lung details more visible. Data augmentation was then used to increase dataset variability prior to model training.

Augmentation (random rotations 5–10°, flips, contrast) increased training data diversity, addressed class imbalance, and reduced overfitting. Only the minority classes, tuberculosis and

pneumonia, were augmented, producing 4,379 new TB images and 1,878 new pneumonia images to balance all classes. The YOLOv8-cls architecture was used in the classification model. The classification head remained unaltered. While earlier research has demonstrated that CBAM can be merged into YOLOv8's head or backbone to enhance feature extraction, this study only looked at backbone integration, as seen in Figure 2.

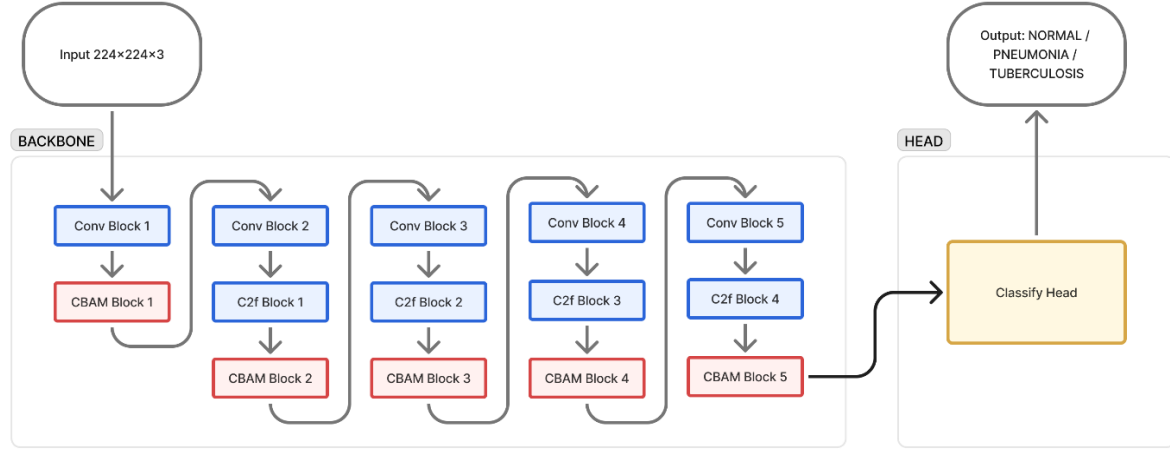


Figure 2. Hybrid architecture of yolov8-cls model with cbam module

YOLOv8's default settings utilized the AdamW optimizer (initial learning rate 0.0014) and Cross Entropy Loss for multiclass classification for 100 epochs and a batch size of 16. Training was carried out on an Apple M4 Pro device with a Metal GPU, 12-core CPU, and 24 GB RAM. Validation was carried out after each epoch, and the checkpoint with the highest validation accuracy was saved. A baseline standard YOLOv8-cls was trained using identical parameters. Performance was measured using accuracy, precision, recall, and F1-score. Accuracy measured correctness, while precision, recall, and F1-score assessed diagnostic errors and balance. Model validity was assessed using an independent test set prepared from the start to prevent data leakage (Zhang et al., 2024).

RESULT AND DISCUSSIONS

Result

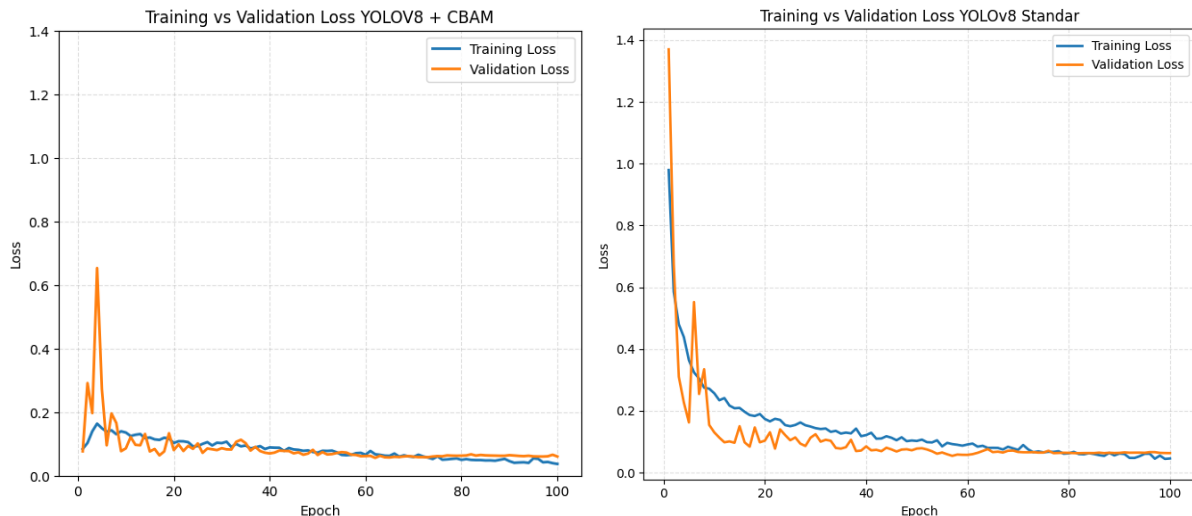


Figure 3. Training loss and validation loss of yolov8+cbam and standard yolov8

The experimental evaluation provides a comprehensive quantitative analysis of the proposed CBAM-infused YOLOv8 architecture, assessing its learning stability and classification performance relative to the standard baseline. Figure 3 shows a comparison of the training loss and validation loss curves between the YOLOv8 with CBAM model and the standard YOLOv8 model during 100 epochs of training. At the beginning of the training process, both models recorded relatively high loss values that sharply decreased within the first ten epochs before reaching stability. In the YOLOv8 with CBAM model, the training loss increased from about 0.08 to 0.16 during the first four epochs, then gradually declined and stabilized around 0.04 toward the end of training. A similar pattern was observed in the validation loss, which started at approximately 0.65 and later stabilized in the range of 0.07 to 0.1 toward the end of training.

Meanwhile, in the standard YOLOv8 model, the initial training loss was around 1.00 and dropped significantly after the first epoch to approximately 0.4, then continued to decrease and stabilized near 0.05 in the final epochs. The validation loss in the standard model initially reached a peak of about 1.36 before decreasing and stabilizing in the range of 0.05 to 0.1. Overall, both models achieved good convergence without any indication of overfitting. The YOLOv8 with CBAM model reached lower training and validation loss values more quickly than the standard YOLOv8 model, indicating faster and more effective learning during the training process.

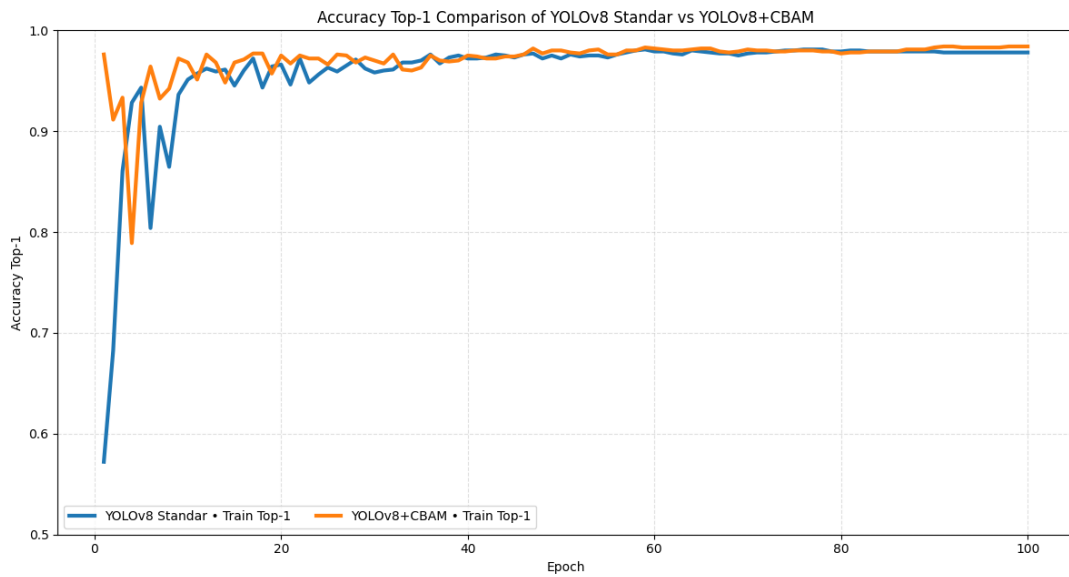


Figure 4. Top-1 validation accuracy of yolov8+cbam and standard yolov8

Figure 4 presents a comparison of the top one accuracy curves on the training data between the standard YOLOv8 model and the YOLOv8 with CBAM model over 100 epochs. Both models showed a rapid increase in accuracy during the early training stages before reaching stability in the later epochs. The YOLOv8 with CBAM model exhibited a similar upward trend but with greater initial fluctuation. Its accuracy briefly dropped to around 79% at the beginning of training and then increased consistently, remaining higher than the standard model after about the twentieth epoch, with a peak accuracy of 98.5%. The standard YOLOv8 model started training with an accuracy of about 56%, then rose sharply to above 90% in the early epochs and remained stable at a high level until the end of training, with the highest accuracy recorded at 98.1%.

Table 1. Comparison of model performance on the test dataset

Model	Test Accuracy	Precision	Recall	F1-score
YOLOv8+CBAM	98.99%	98.71%	98.43%	98.57%
YOLOv8	97.37%	97.56%	97.45%	97.50%

Table 1 presents the testing results of the YOLOv8 with CBAM model and the standard YOLOv8 model on the test dataset. Overall, the YOLOv8 with CBAM model demonstrated higher performance than the standard YOLOv8 model across all evaluation metrics. The YOLOv8 with CBAM model achieved an accuracy of 98.99%, with a precision of 98.7%, a recall of 98.43%, and an F1-score of 98.57%. Meanwhile, the standard YOLOv8 model obtained an accuracy of 97.37%, with a precision of 97.56%, a recall of 97.45%, and an F1-score of 97.50%. Both models performed well overall, but the increases of about 1.62% in test accuracy, 1.15% in precision, 0.98% in recall, and 1.07% in F1-score achieved by the YOLOv8 with CBAM model indicate a positive effect of CBAM integration on model performance. These findings are consistent with the attention mechanism theory, where the combination of channel and spatial attention in CBAM helps the model focus on relevant lung areas while suppressing non-informative features.

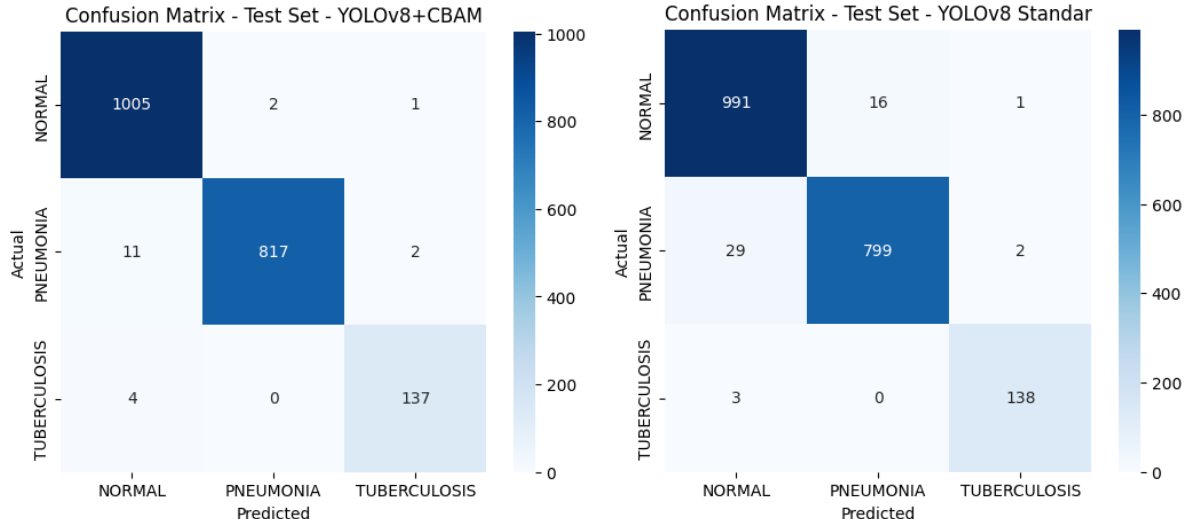
**Figure 5.** Comparison of confusion matrices of yolov8+cbam and standard yolov8

Figure 5 presents a comparison of the confusion matrices on the test dataset between the YOLOv8 with CBAM model and the standard YOLOv8 model. In the YOLOv8 with CBAM model, out of 1008 normal images, 1005 were correctly classified, with only two images misclassified as pneumonia and one as tuberculosis. Out of 830 pneumonia images, 817 were correctly identified, while eleven were misclassified as normal and two as tuberculosis. For the tuberculosis class, out of 141 images, 137 were correctly classified, four were incorrectly predicted as normal, and none were mistaken for pneumonia.

In the standard YOLOv8 model, performance remained high but slightly lower. Out of 1008 normal images, 991 were correctly classified, sixteen were predicted as pneumonia, and one as tuberculosis. Out of 830 pneumonia images, 799 were correctly classified, twenty-nine were misclassified as normal, and two as tuberculosis. Out of 141 tuberculosis images, 138 were correctly classified and three were misclassified as normal. Overall, the YOLOv8 with CBAM model produced a higher number of correct classifications and fewer interclass misclassifications compared with the standard YOLOv8 model.

Discussions

The observed rapid convergence and stability (Figures 3 and 4) can be attributed to the attention mechanism's ability to dynamically recalibrate feature maps. Consistent with the foundational principles of CBAM, the module sequentially infers attention maps to effectively suppress irrelevant background information while amplifying meaningful features (Guo et al., 2022; Yan et al., 2024). In the specific context of chest radiography, standard CNN backbones often struggle to differentiate between pathological signs and anatomical noise, such as ribs or clavicles. By employing spatial attention, the proposed model can down-weight these non-informative background regions early in the training phase. This enables the network to update its weights more efficiently, focusing specifically on gradients associated with pulmonary abnormalities rather than wasting computational resources on anatomical artifacts.

With respect to classification performance on the test set (Table 1), the results confirm that integrating attention mechanisms significantly enhances predictive capability, achieving a top accuracy of 98.99%. This improvement aligns with recent findings in medical imaging, which suggest that the 'dual-focus' nature of CBAM is critical for distinguishing fine-grained patterns (Oladimeji & Ibitoye, 2023). The Channel Attention module prioritizes 'what' the feature is allowing the model to detect subtle textural variations like the consolidations found in pneumonia. Simultaneously, the Spatial Attention module focuses on 'where' the feature is located, directing the network toward lung fields where lesions manifest. This synergy allows the model to capture complex pathological details that standard architectures might miss, effectively reducing diagnostic uncertainty (Priambodo & Fatichah, 2025).

Crucially, the examination of diagnostic errors via confusion matrices (Figure 5) highlights a substantial reduction in misclassifications, particularly for pneumonia cases. The standard YOLOv8 model misclassified 29 pneumonia images as normal, whereas the CBAM-infused model reduced this to only 11. This reduction addresses the critical challenge of 'overlapping visual patterns' described by Pal et al. (2024), where subtle pneumonia infiltrates often resemble normal physiological markings. By refining the feature extraction process, the attention mechanism effectively enhances the contrast between pathological lesions and healthy tissue, thereby resolving ambiguous cases that standard models fail to detect.

The clinical implication of minimizing these False Negatives is profound. As highlighted in recent epidemiological studies by Firdaus et al. (2025), undiagnosed respiratory infections are a primary driver of disease transmission and mortality in high-burden regions like Indonesia. A diagnostic tool that significantly lowers the rate of missed diagnoses offers a higher degree of safety and reliability. Consequently, the proposed model's ability to salvage these 'borderline' cases makes it exceptionally well suited for deployment in mass screening workflows where sensitivity is paramount.

The proposed X-RayVision-Net demonstrates a marked advancement in diagnostic capability relative to established baselines in the field. While standard CNN architectures have achieved approximately 94% accuracy in similar pulmonary tasks (Susanti et al., 2023), and standard YOLOv8 implementations in other medical domains typically range between 92% and 94% (Khalaf & Abdulateef, 2024; Muhashin & Stefanie, 2024), our hybrid model approached 99% accuracy. This aligns with recent studies suggesting that attention mechanisms are essential for breaking the performance ceiling of standard CNNs, similar to the 98.97% accuracy reported by Priambodo & Fatichah (2025) in dermatology. However, our study extends this validation specifically to the domain of chest radiography, confirming that the synergy between YOLOv8's rapid inference and CBAM's feature refinement is highly effective for visualizing complex lung pathologies.

This study provides contributions in both theoretical and practical dimensions. From a theoretical perspective, it introduces and validates a hybrid deep learning architecture that effectively balances computational efficiency and diagnostic sensitivity. From a practical

standpoint, the proposed model functions as a reliable decision-support system that can assist clinicians by providing a “second opinion,” particularly in resource-limited settings such as Indonesia, where the availability of radiologists remains constrained. Furthermore, the integration of CLAHE and balanced data augmentation enhances the model’s robustness to variability in chest X-ray image quality, a common challenge in real-world clinical environments.

This study recognizes several constraints related to its experimental design and scope. The evaluation was conducted using publicly available datasets which, despite their diversity, may not fully represent the noise patterns and acquisition artifacts commonly encountered in real-time clinical imaging. In addition, although the proposed model demonstrates strong predictive performance, it does not natively provide visual interpretability of its decision-making process. Future investigations should therefore prioritize validation on external, multi-center clinical datasets to strengthen evidence of generalizability. Moreover, the integration of explainability approaches, such as Gradient-weighted Class Activation Mapping (Grad-CAM), is recommended to generate attention maps that enable clinicians to confirm that the model’s predictions are driven by relevant pulmonary regions rather than extraneous or confounding image features.

CONCLUSION

This study successfully establishes the efficacy of integrating the CBAM into the YOLOv8 architecture, demonstrating a substantial advancement in the automated classification of pulmonary diseases. Quantitative analysis reveals that the proposed model achieved an accuracy of 98.99%, representing a net improvement of 1.62% over the standard YOLOv8 baseline, alongside consistent gains in precision, recall, and F1-score. These findings corroborate the theoretical premise that combining channel and spatial attention mechanisms significantly refines feature representation, thereby enhancing the model’s capacity to differentiate the complex radiographic patterns of pneumonia and tuberculosis. The clinical utility of this model is underscored by its potential to minimize diagnostic errors, theoretically preventing approximately sixteen missed diagnoses per thousand cases compared to the baseline. To ensure broader clinical applicability, future work should focus on validating the model using multi-center datasets and incorporating qualitative assessments from radiologists. The primary contribution of this work lies in providing the first targeted evaluation of the YOLOv8-CBAM synergy for rapid and accurate chest X-ray categorization.

REFERENCES

Alfaqeeh, M., Ewart, S., Tanoto, R., Buenastuti, W., Istorini, I. A., Yosephine, P., Burhan, E., Siagian, R. C., Hadinegoro, S. R., Lenggogeni, D., White, R. G., Suwantika, A. A., Kasaeva, T., & Giersing, B. (2025). New adult and adolescent tuberculosis vaccines and Indonesia: policy planning and evidence, November 2024. *Vaccine*, 62, 127490. <https://doi.org/10.1016/j.vaccine.2025.127490>

Alzubaidi, L., Zhang, J., Humaidi, A. J., Al-Dujaili, A., Duan, Y., Al-Shamma, O., Santamaría, J., Fadhel, M. A., Al-Amidie, M., & Farhan, L. (2021). Review of deep learning: concepts, CNN architectures, challenges, applications, future directions. *Journal of Big Data*, 8(1). <https://doi.org/10.1186/s40537-021-00444-8>

Ciptaningtyas, V. R., Sumekar, T. A., Fauzia, L. P., Lestari, E. S., Farida, H., Margawati, A., de Mast, Q., & de Jonge, M. I. (2025). Community-acquired pneumonia in Indonesian children: insights into diagnosis, treatment compliance, and healthcare provider challenges. *Archives of Public Health*, 83(1), 1–12. <https://doi.org/10.1186/s13690-025-01795-x>

Firdaus, Y., Nasution, S. K., & Juanita. (2025). Public-Private Mix Strategy for Tuberculosis

Control in Medan: A Qualitative Descriptive Study. *International Journal of Health, Education & Social (IJHES)*, 8(6), 106–122.

Guo, M. H., Xu, T. X., Liu, J. J., Liu, Z. N., Jiang, P. T., Mu, T. J., Zhang, S. H., Martin, R. R., Cheng, M. M., & Hu, S. M. (2022). Attention mechanisms in computer vision: A survey. *Computational Visual Media* 2022 8:3, 8(3), 331–368. <https://doi.org/10.1007/s41095-022-0271-y>

Hadhoud, Y., Mekhaznia, T., Bennour, A., Amroune, M., Kurdi, N. A., Aborujilah, A. H., & Al-Sarem, M. (2024). From Binary to Multi-Class Classification: A Two-Step Hybrid CNN-ViT Model for Chest Disease Classification Based on X-Ray Images. *Diagnostics*, 14(23), 2754. <https://doi.org/10.3390/diagnostics14232754>

Hekmatyar, H. D., Saputra, W. A., & Ramdani, C. (2022). Klasifikasi Pneumonia Dengan Deep Learning Faster Region Convolutional Neural Network Arsitektur VGG16 dan ResNet50. *InComTech : Jurnal Telekomunikasi Dan Komputer*, 12(3), 186. <https://doi.org/10.22441/incomtech.v12i3.15112>

Karim, A. H. M. Z., Chowdhury, T., Bil, K., Mahmud, O., Khanam, F., Rahman, K. M. A., & Fahima, R. A. (2024). COVID-19, Pneumonia, and Healthy Lungs Classification Using CNN and Transfer Learning Model Using Chest X-Ray. *American Journal of Biomedical Engineering*, 12(1), 1–6.

Khalaf, A. T., & Abdulateef, S. K. (2024). Ophthalmic Diseases Classification Based on YOLOv8. *Journal of Robotics and Control (JRC)*, 5(2), 408–415. <https://doi.org/10.18196/jrc.v5i2.21208>

Muhlashin, M. N. I., & Stefanie, A. (2024). Eye Disease Classification Based On Fundus Image Using Yolo V8. *Jurnal Media Computer Science*, 3(1), 33–40. <https://doi.org/10.37676/jmcs.v3i1.4572>

Nunes, J. C. S., Linhares, J. E. B. de S., Postigo, M. A. O., Rio, D. G. d., Sobrinho, A. M. F., & Torné, I. G. (2025). Cancer Cell Classification from Peripheral Blood Smear Data Using the YOLOv8 Architecture. *IEEE Access*, 13, 91911–91924. <https://doi.org/10.1109/ACCESS.2025.3573277>

Oladimeji, O. O., & Ibitoye, A. O. J. (2023). Brain tumor classification using ResNet50-convolutional block attention module. *Applied Computing and Informatics*, 20(1/2), 1–17. <https://doi.org/10.1108/ACI-09-2023-0022>

Pal, V., Pabari, H., Indoria, S., Patel, S., Krishnan, D., & Ravi, V. (2024). Multifaceted Disease Diagnosis: Leveraging Transfer Learning with Deep Convolutional Neural Networks on Chest X-Rays for COVID-19, Pneumonia, and Tuberculosis. *The Open Bioinformatics Journal*, 17(1). <https://doi.org/10.2174/0118750362303182240516043224>

Pradeepa, R., Punitha, V., & Senthamil Selvi, R. (2024). Deep Learning Algorithms for Skin Disease Classification. *Journal of Innovative Image Processing*, 6(2), 84–95. <https://doi.org/10.36548/jiip.2024.2.001>

Priambodo, A. R., & Faticah, C. (2025). Leveraging Convolutional Block Attention Module (Cbam) For Enhanced Performance In Mobilenetv3-Based Skin Cancer Classification. *Jurnal Teknik Informatika (Jutif)*, 6(3), 1389–1404. <https://doi.org/10.52436/1.jutif.2025.6.3.4546>

Susanti, L. A., Soleh, A. M., & Sartono, B. (2023). Deep Learning Image Classification Rontgen Dada pada Kasus Covid-19 Menggunakan Algoritma Convolutional Neural Network. *Jurnal Teknologi Informasi Dan Ilmu Komputer*, 10(5), 973–982. <https://doi.org/10.25126/jtiik.2023107142>

Suvvari, T. K. (2025). The persistent threat of tuberculosis – Why ending TB remains elusive? *Journal of Clinical Tuberculosis and Other Mycobacterial Diseases*, 38, 100510. <https://doi.org/10.1016/j.jctube.2025.100510>

Theotokis, P. (2025). Human Brain Inspired Artificial Intelligence Neural Networks. *Journal*

of Integrative Neuroscience, 24(4), 26684. <https://doi.org/10.31083/JIN26684>

Umar, K. F., Noor, N. N., Maria, I. L., Bustan, M. N., Abdullah, M. T., & Thaha, R. M. (2024). Risk Factor of Paediatric Community-Acquired Pneumonia in Wajo Regency, Indonesia. *National Journal of Community Medicine*, 15(02), 98–104. <https://doi.org/10.55489/njcm.150220243601>

Yan, J., Zeng, Y., Lin, J., Pei, Z., Fan, J., Fang, C., & Cai, Y. (2024). Enhanced object detection in pediatric bronchoscopy images using YOLO-based algorithms with CBAM attention mechanism. *Helijon*, 10(12), e32678. <https://doi.org/10.1016/j.helijon.2024.e32678>

Yu, X., Yang, X., Song, Y., Yu, J., Jiang, T., Tang, H., Yang, X., Zeng, X., Bi, J., Shen, A., & Sun, L. (2025). Lower respiratory tract co-infection of Streptococcus pneumoniae and respiratory syncytial virus shapes microbial landscape and clinical outcomes in children. *Frontiers in Cellular and Infection Microbiology*, 15. <https://doi.org/10.1016/j.helijon.2024.e32678>

Zhang, P., Sanida, M. V., Sanida, T., Sideris, A., & Dasygenis, M. (2024). An Advanced Deep Learning Framework for Multi-Class Diagnosis from Chest X-ray Images. *J*, 7(1), 48–71. <https://doi.org/10.3390/J7010003>

